HEFAT2012
9th International Conference on Heat Transfer, Fluid Mechanics and Thermodynamics
16 – 18 July 2012
Malta

THERMOREFLECTANCE SMALL SCALE TEMPERATURE MEASUREMENT UNDER AMBIENT CONDITIONS

Drazen Fabris[1,2,*], Christopher Cardenas[1,2], Shawn Tokairin[1,2], Patrick Wilhite[1] and Cary Y. Yang[1,3]
*Author for correspondence
[1]Center for Nanostructures, Santa Clara, California 95053, USA
[2]Department of Mechanical Engineering,
[3]Department of Electrical Engineering,
Santa Clara University,
Santa Clara, California 95053,
USA
E-mail: dfabris@scu.edu

ABSTRACT

Thermoreflectance is a non-contact method to measure temperature on small scales which utilizes the temperature dependent change in normal reflectance of the surface under a probe light source. The sensitivity to the temperature change is determined by the thermoreflectance coefficient which is considered linear and calibrated over the temperature range to be studied. The current experiments conducted in an ambient environment show that the thermoreflectance coefficient exhibits a hysteresis with the first calibration and the hysteresis returns after several days. Under LED illumination centered about 535 nm the thermoreflectance coefficient is shown to change from -1.69×10^{-5} to -1.77×10^{-4} $^{o}C^{-1}$ whereas under wavelengths centered about 494 nm the thermoreflectance coefficient changes from 2.13×10^{-4} to -2.31×10^{-5} $^{o}C^{-1}$. The hypothesized cause of the hysteresis is water adsorption from the ambient laboratory environment.

INTRODUCTION

In electronics and other applications there is a need to measure temperature on small scales and with non-contact methods. Future chip designs rely on a better understanding of heating and performance of materials and electric circuits *in-situ*. Specifically in interconnects and vias, the metallic grain size decreases with feature size which thereby reduces electrical conductivity [1]. At the same time thermal conductivity decreases with feature size and contact resistance between the conductor and substrate increases. If current density is kept the same, this leads to increased local heating in chips and a greater potential for failure.

There currently exist a large number of temperature measurement techniques that bridge from very small scales, thermal atomic force microscopy (TAFM) and micro Raman, to traditional larger scale thermocouple and infrared measurements. While each of these techniques has its benefits, few methods allow for both small scale and non-contact full field measurement. Thermoreflectance and other optical (non-contact) methods to measure temperature are surveyed by Christofferson, *et al.* [2]. Thermoreflectance is a technique by which the temperature of a sample can be measured through the change in reflectance of the material [3]. The technique benefits from the ability to use a CCD array and optical microscope to obtain a full field measurement and can be applied in-situ [4]. Unlike an infrared measurement, the technique employed uses a white light source or narrow band LED to probe the surface, which enables both smaller scale measurements due to a shorter wavelength and a stronger signal at low temperatures.

To successfully determine temperature, the thermo-reflectance coefficient needs to be calibrated for the specific material to be studied. The precise behavior of the material will depend on the purity, crystallinity, surface morphology, thickness, and any adsorbed molecules on the surface. This calibration requires the entire sample to be heated through the range of temperatures measured and the reflectance measured at the wavelengths of interest. The thermoreflectance coefficient obtained by uniformly heating a multi-layer transparent sample may consist of contributions to the temperature dependence of overall reflectance from the interfacial reflectances [5] which may differ from the thermoreflectance signal when the system is Joule or pump laser heated. The calibration is typically done under an ambient environment and starting at ambient temperature. The calibrated coefficient is compared to published values to demonstrate consistency in the result. During the calibration, we have determined a hysteresis of the thermoreflectance coefficient. This difference in thermoreflectance coefficient can lead to dramatically different results if the system is not calibrated properly. The effect is consistent with an adsorbed layer of water.

NOMENCLATURE

I	[W/m^2] or arbitrary units [AU]	Intensity
t	[sec]	Time
T	[^{o}C]	Temperature
V	[Volts]	Voltage

Special characters

λ	[nm]	Wavelength of light
κ	[^{o}C^{-1}]	Thermal reflectance coefficient
ρ	[-]	Reflectivity

Subscripts

0	Reference state
1/2	Half width
Meas.	Measured
n	Normal direction

THERMOREFLECTANCE

The thermoreflectance technique relies on a calibration of reflectance under specific wavelengths over the temperature range in question. The normal spectral reflectance intensity at a given temperature, $I_n(T)$, is proportional to the normal spectral reflectance, $\rho_n(T)$, and is acquired under constant spectral illumination, I_0

$$I_n(T) = \rho_n(T) I_0 . \tag{1}$$

The spectral thermoreflectance coefficient is defined by the normalization of the slope as a function of temperature with the reference quantity

$$\kappa = \frac{1}{\rho_n(T_0)} \frac{\partial \rho_n}{\partial T} = \frac{1}{I_n(T_0)} \frac{\partial I_n}{\partial T} \tag{2}$$

where κ is the spectral TR coefficient (^{o}C^{-1}). The temperature difference is obtained with measurements for the thermoreflectance coefficient and the relative intensity change as a function of temperature

$$\Delta T = \left(\frac{I_n(T) - I_n(T_0)}{I_n(T_0)} \right) \frac{1}{\kappa} \tag{3}$$

where $\Delta T = (T - T_0)$ is the temperature difference (^{o}C). The sensitivity of the thermoreflectance coefficient, κ, is typically 10^{-4} ^{o}C^{-1}; hence, a very robust measurement is required for accuracy [6]. The temperature dependence of the normal spectral reflectance is typically linearized over the range of temperature to be measured.

The thermoreflectance technique has been used by the authors to measure the temperature of model gold interconnects [7] shown in Figure 1. In these experiments a current is passed through a 1 μm wide, 100 nm thick, and 20 μm long gold line. The amount of local heating is based on the current passed through the line and thermal conduction to the substrate. Peak temperatures of 200 ^{o}C have been measured. Using this technique combined with a numerical model of thermal transport, it is possible to measure the thermal contact resistance between the interconnect line and the substrate [8]. The results are consistent with extrapolations from other measurements of contact resistance [9]. The experiments considered illumination at four different wavelengths and interconnect lines of different lengths.

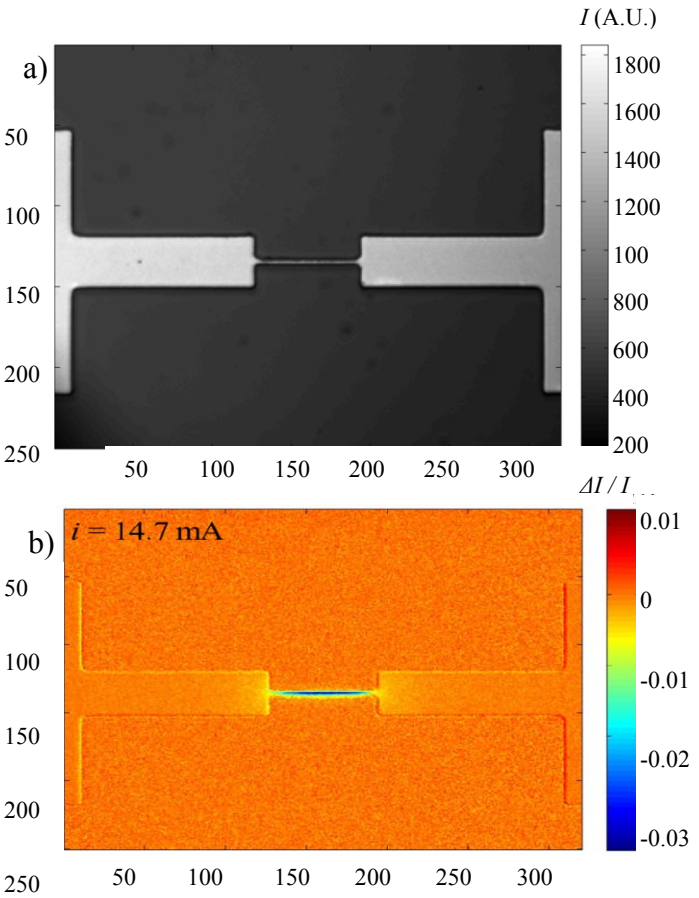

Figure 1 Microscopic image of gold interconnect structure (a), and thermal reflectance signal under self heating (b). The gold structure is 20 μm long and 1 μm wide at the narrowest section, $\lambda_{Meas.}$ = 535 nm. The images are measured in pixels. The self heating signal is shown in the relative change in intensity.

EXPERIMENT

The experiment and the calibration use a gold thin film which was designed for carbon interconnect research and as a reference control measurement [10]. The interconnect substrate consists of several layers shown in Figure 2. The substrate stack from lowest to top is composed of a silicon wafer followed by a deposited amorphous SiO_2 insulation layer with a 10 nm titanium adhesion layer in contact with the gold. The interconnect layout consist of two pads used for landing low

impedance electrical probes, thin film leads, and a narrow test line connecting the leads. The surrounding darker region is the SiO_2 oxide and the reflection off the darker silicon substrate. Fabrication of the line length was systematically varied from 1 to 50 µm. For calibration, larger gold structures were used to provide an increased area to determine the reflectance signal. A K-type thermocouple is used to provide a reference temperature measurement of the surface.

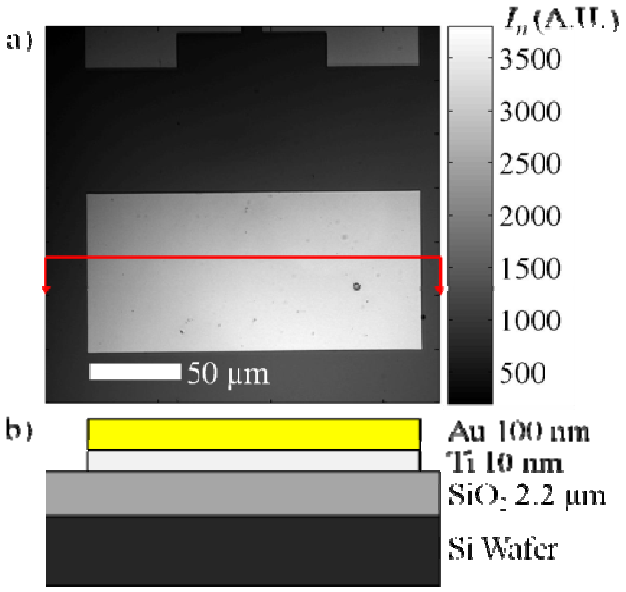

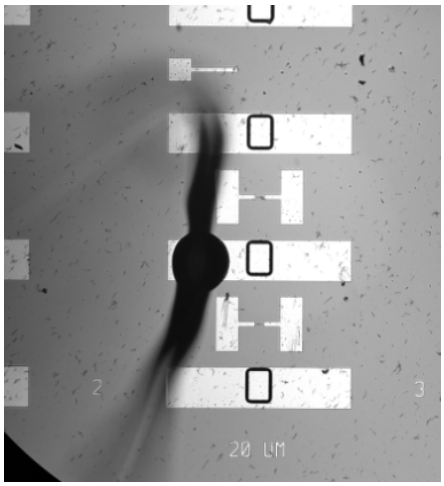

Figure 1 Thin film gold samples. a) Reflectance intensity image gathered under $\lambda_{Meas.}$ = 535 nm. b) Substrate layers and thicknesses, and c) 35 micron K-type thermocouple placed on the surface.

The thermoreflectance apparatus is shown in Figure 3. It consists of a high power optical microscope, a heated sample holder, electrical probes, a LED, a CCD, probe station, and acquisition equipment. The samples are interrogated with Philips LUXEON® Star/O LED illumination. The LED characteristics indicating the peak emission wavelength, λ_{Peak}, and spectral half width, $\Delta\lambda_{1/2}$, can be found in Table 1. LED spectral emission distributions were measured with an Ocean Optics USB 2000 in place at the location of samples.

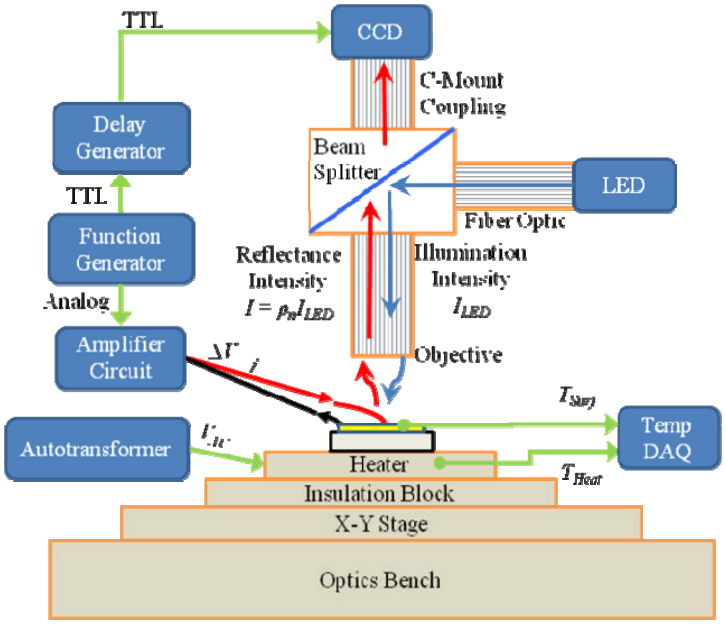

Figure 3 Thermoreflectance system schematic. The sample is illuminated with narrow bandwidth light the reflected signal is collected through a microscopic objective.

Table 1 Manufacturer model number of LED corresponding with the manufacturer specified peak emission wavelength ($\lambda_.$), measured peak emission wavelength ($\lambda_{Meas.}$), and spectral line half width ($\Delta\lambda_{1/2}$).

Model Number	λ (nm)	$\lambda_{Meas.}$ (nm)	$\Delta\lambda_{1/2}$ (nm)
LXHL-NRR8	455	446	26
LXHL-NB98	470	458	26
LXHL-NE98	505	494	26
LXHL-NM98	530	535	31

A Prosilica Inc. CCD (GE1380) images the system through a modified Meiji Techno microscope Series MC-50T with objectives of 5 to 50 times magnification. The sensor array is a 1024 x 1360 Sony ICX285AL 16-bit CCD and transfers data by progressive interline scanning. Individual pixel size is specified at 6.45 x 6.45 µm^2. At full resolution, the maximum frame rate is 20.2 fps. The digitization utilizes the GigE Vision Standard 1.0 software protocol for interfacing with the network adapter. The A/D conversion is performed internally with 12-bit accuracy and therefore data is further quantized from the sensor's 16-bit actual level. The experimental apparatus has a custom built heated stage with micrometers used for manual controlled positioning. The entire system is placed on an optical table to reduce vibrations.

The experiments such as those shown in Figure 1 consist of capturing a consecutive series of images while the system is alternately in a heated and cooled state. The time sequence of

the data capture is shown in Figure 4. Since the structures are very small, the transient heating time is very short and the system is in a quasi-steady state (transient time is estimated to be 25 ms). During the experimental measurement, acquisition of repeated hot and relaxed sample images acts to average the long-time fluctuations in the illumination and other environmental variables. Acquisition of measurement data are typically achieved for 4,000 total frames over the duration of several minutes.

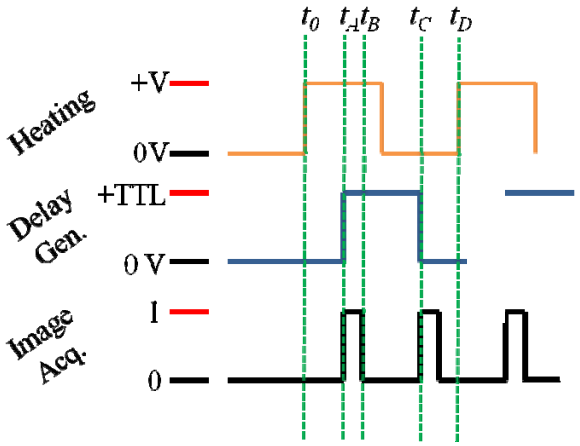

Figure 4 Heating, delay, and image acquisition timing signals for quasi-steady lock-in thermoreflectance imaging, t_0 is the initial rising edge of the function generator used. A digital delay generator is used to stagger the image acquisition to alternate between heated and cooled images.

The thermoreflectance calibration coefficient is not widely available in literature and possible variation with film thickness, light source characteristics, and material properties, necessitate calibration for the samples to be tested. In the calibration and experiments conducted, the 100 nm thick gold film is not expected to show substantial thermal expansion, but any contribution is systematically captured in the measurements [11]. During the calibration, the sample is first heated to beyond 200 ^{o}C and then progressively cooled. Measurements are taken at multiple steady-state temperatures during the cooling. The heated sample stage enables fixed temperature control to achieve a thermal steady state (+/- 0.3 ^{o}C). Surface temperature was measured with a small surface deposited thermocouple, wire diameter < 13 µm. Following acquisition, the thermoreflectance coefficient was then calculated by use of Equation 2.

RESULTS

Data were obtained for two samples under two different LEDs (535 nm and 494 nm) over regions of gold, Figure 5. Both data sets were obtained for first increasing then decreasing the system temperature. The time required to achieve a thermal steady state was 40 minutes and the data are recorded for 10 minutes. At an illumination at 535 nm the initial value of the thermoreflectance coefficient is -1.69 x 10^{-5} ^{o}C^{-1} which is an order of magnitude smaller that the value after the initial heating cycle, -1.77 x 10^{-4} ^{o}C^{-1}. The second calibration is during the cooling cycle. Under the second illumination wavelength, 494 mn, the thermoflectance coefficient is also seen to change sign in addition to the magnitude changing. In this calibration, only one initial point is measured prior to the first heating cycle.

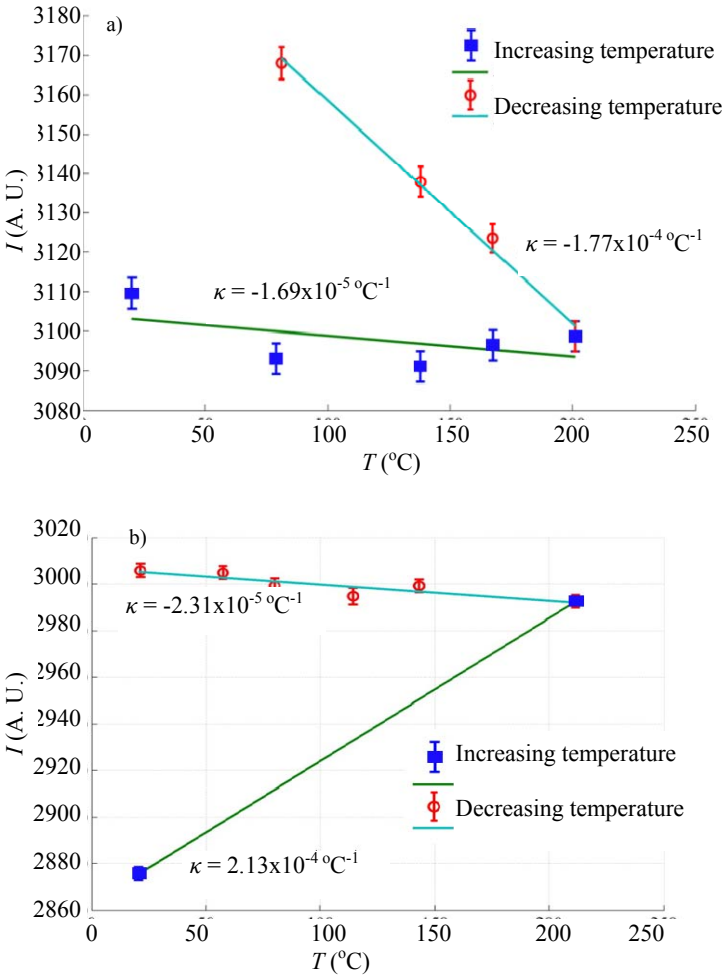

Figure 5 Temperature dependence of the reflectance intensity. a) Under $\lambda_{Meas.}$ = 535 nm. b) Under $\lambda_{Meas.}$ = 494 nm. Error bars represent standard deviation of the means to 95% confidence.

Figure 6 shows the calibration data for the oxide region at 494 nm. In this case the light is reflecting off the silicon wafer beneath. The experiment was initially started at ambient temperature then heated to 211 ^{o}C and then the remainder of the calibration points was taken. The corresponding gold calibration is shown in Figure 5b.

The reflectance intensity data exhibits a linear relationship with temperature in the repeatable regime, following heating to beyond 200^{o}C. The thermoreflectance coefficient calculated by the temperature dependence of the response clearly changes prior to and following heating to beyond 200^{o}C. The temperature required to fully desorb the hypothesized film layer has not been determined, but the consistency of the calibrations for subsequent heating and cooling cycle indicates that the

system is in stable state, Figure 7. It can be seen that after leaving the system overnight some reduction of reflectance intensity is observed but the thermoreflectance coefficient does not change. Following the acquisition of the data contained in Figure 5b, measurements in Figure 8 indicate that the reflectance intensity decreases with time and may approach or pass the initial reflectance.

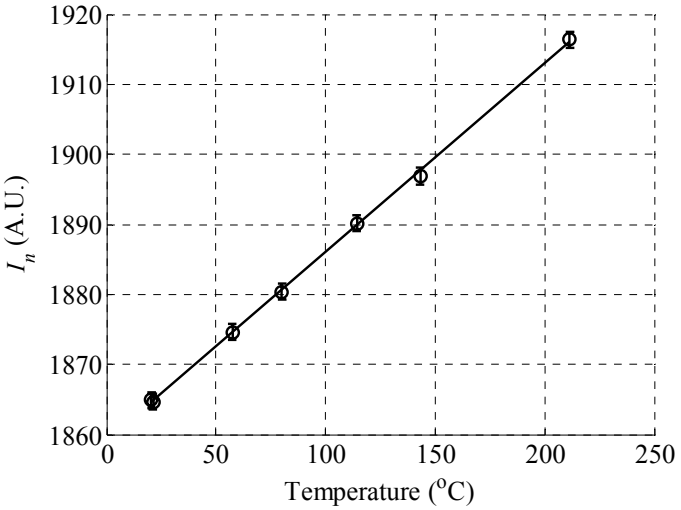

Figure 6. Thermoreflectance calibration for region covered with SiO_2 under $\lambda_{Meas.}$ = 494 nm. The oxide is optically thin and the reflectance is based on the silicon wafer substrate.

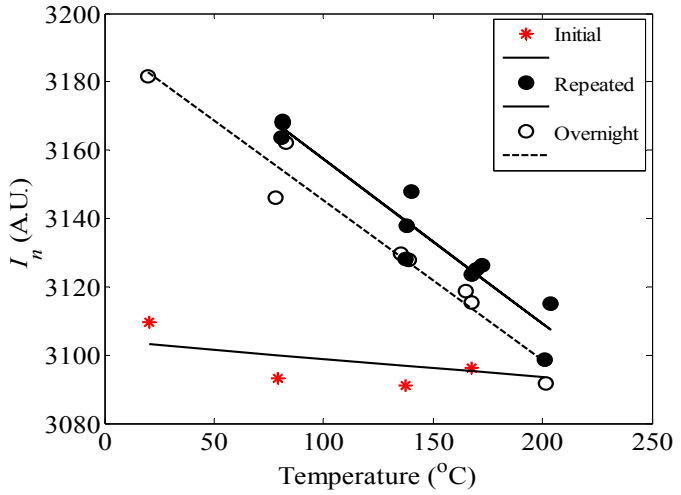

Figure 7 Repeated measurements after an initial heating cycle. The secondary and subsequent heating and cooling cycles follow the same behavior as the first cooling cycle.

The calibration data acquisition reflectance intensity measurements were taken for over 640 hours at ambient temperature as shown in Figure 8. The reflectance intensity measurements were normalized to the maximum values contained in multiple square regions of gold (6 regions of 3.1 μm^2) and SiO_2 (3 regions of 3.1 μm^2). During this period the relative humidity varied from 38 to 78% and averaged about 65%. The humidity was not controlled in the lab.

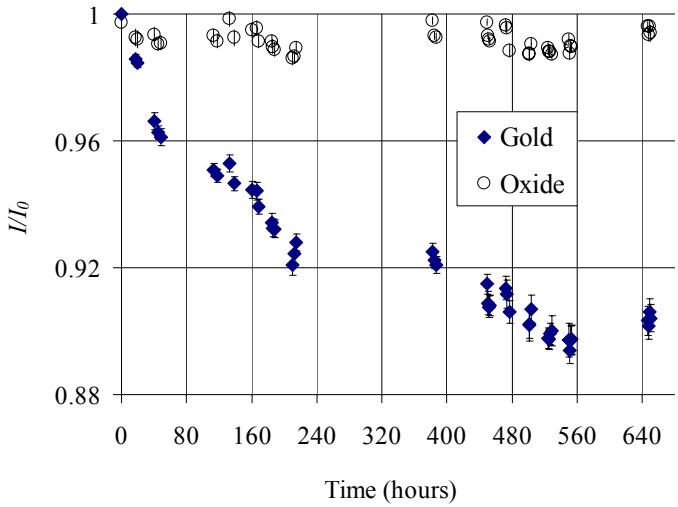

Figure 8 Time dependent normalized reflectance intensity signal under $\lambda_{Meas.}$ = 494 nm. Data were acquired at ambient temperature following a thermal cycle to above 200 ^{o}C.

The hysteresis behavior exists for the gold regions for both wavelengths tested, while the hysteresis is not observed for the regions covered by oxide. It is well known that water will form a double layer on metallic surfaces. At low temperature bilayer ice particles have been studied adsorbing to the metallic surfaces. In the instance of gold, it has been shown that a hexagonally bonded ring of water molecules will orient with the gold lattice at the surface with four or five free O-H bonds orienting towards the surface [12]. This difference in attraction with O and H atoms has as also been observed in molecular dynamics simulations and shown to produce a preferential location of water molecules up to two molecules thick, 6-8 Å [13]. Although adsorption in an ice form has been seen over a cryogenic range, water adsorption has also been measured at ambient temperatures under both atmospheric conditions, Lee and Staehle [14], and under high vacuum, Wells [15]. In the Lee and Staehle study, the water adsorption was measured through the change in mass of the system using an ultrasensitive resonance balance. The rate of adsorption was found to be related to the relative humidity and to occur on a time scale of 3 hours or longer. In the Wells work, the adsorption layer was shown to change the work function of the surface (the energy potential required to raise an electron off the surface). Since the absorbed layer changes the electron energy states, it is then not surprising that it will also affect the reflectivity.

The data show good agreement to the two published measurements [7, 16] in Figure 9. Wavelength weighted predictions of the thermoreflectance calibration coefficients have been included for comparison to the data. The weighted average computation utilizes the spectral sensitivity of the CCD, illumination distribution of each LED, and the laser based calibration reported in [9]. Compared to the laser based method, the data demonstrate the correct trend with a decrease

in the magnitude due to the spectral width of the LEDs and CCD readout sensitivity. The method reported by Beran made use of a monochromator bandwidth of 6 nm reducing the spectral averaging and more closely matching the data of Burzo. Uncertainty in the thermoreflectance coefficient of gold is measured with 95% confidence based on the variation in the collected data. Significant contributions to systematic error include uncertainty in the thermocouple temperature measurement (< 0.3 °C), local spatial variation of intensity (< 0.12%), and repeated mean intensity variation (< 0.76%). The overall uncertainty in the thermoreflectance calibration coefficient under LED illumination is +/-15%.

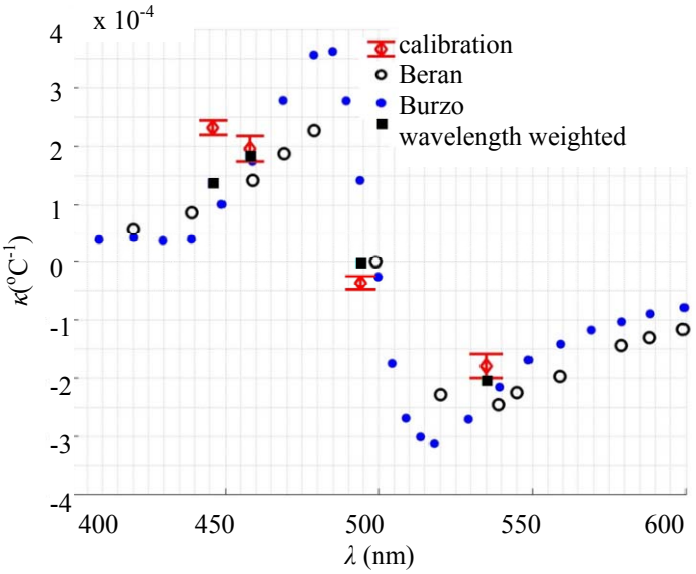

Figure 9 Thermoreflectance calibration under LED illumination. Data from Beran [16] and Burzo *et al.* [9] are included for comparison of results for similar techniques on similar structures.

CONCLUSIONS

Hysteresis of the metallic thermoreflectance calibration with increasing and decreasing sample temperature has been observed. The hysteresis is believed to be due to water adsorption at the surface. The water is removed when the sample is heated and the calibration is repeatable. The adsorbed layer returns after several days. Under some illumination wavelengths, the sign of the thermoreflectance calibration coefficient may change and the magnitude is significantly different. The thermoreflectance coefficient is equivalent to the spectrally weighted published thermoreflectance calibration data based on pump-probe techniques.

ACKNOWLEDGEMENTS

The authors would like to thank Francisco Madriz for fabrication of the gold thin film samples. This work was supported by the United States Army Space and Missile Defense Command (SMDC) and carries Distribution Statement A, approved for public release, distribution unlimited.

REFERENCES

[1] Steinhögl, W., Schindler, G., Steinlesberger, G., Traving, M., and Engelhardt, M., Comprehensive study of the resistivity of copper wires with lateral dimensions of 100 nm and smaller, *J. Appl. Phys.,* Vol. 97, 2005, paper 023706.

[2] Christofferson, J., Maize, K., Ezzahri, Y., Shabani, J., Wang, X., and Shakouri, A., Microscale and nanoscale thermal characterization techniques, *Thermal Issues in Emerging Technologies,* Cairo, Egypt, pp. 3-9, 2007.

[3] Farzaneh, M., Maize, K., Lüerßen, D., Summers, J. A., Mayer, P. M., Raad, P. E., Pipe, K. P., Shakouri, A., Ram, R. J., and Hudgings, J. A., TOPICAL REVIEW: CCD-based thermoreflectance microscopy: principles and applications, *J. Physics D: Applied Physics,* Vol. 42, 2009, paper 143001.

[4] Grauby, S., Dilhaire, S., Jorez, S., and Claeys, W., Imaging setup for temperature, topography, and surface displacement measurements of microelectronic devices, *Review of Scientific Instruments,* Vol. 74, 2003, pp. 645-647.

[5] Siegel, R. and Howell, J. *Thermal Radiation Heat Transfer,* (Chapter 18), 4th ed., Taylor & Francis, New York, 2002.

[6] Komarov, P.L., Burzo, M.G., and Raad, P.E., A thermoreflectance thermography system for measuring the transient surface temperature field of activated electronic devices, *Semiconductor Thermal Measurement and Management Symposium, 2006 IEEE Twenty-Second Annual IEEE*, pp. 199-203, 2006.

[7] Cardenas, C.V., Thermoreflectance Temperature Measurement and Application to Gold Thin Films and Carbon Nanofibers, Master's Thesis, 2012, Santa Clara University Department of Mechanical Engineering, Santa Clara, CA 95053.

[8] Cardenas, C. V., Fabris, D., Tokairin, S., Madriz, F., and Yang, C. Y., Thermoreflectance measurement of temperature and thermal resistance of thin film gold, submitted to ASME Journal of Heat Transfer, 2012.

[9] Burzo, M.G., Komarov, P.L., and Raad, P.E., Optimized Thermo-Reflectance System for Measuring the Thermal Properties of Thin-films and Their Interfaces, *22nd Annual IEEE SEMI-THERM Symposium*, pp. 87-94, 2006.

[10] Madriz, F.R., Jameson, J.R., Krishnan, S., Sun, X., and Yang, C.Y., Circuit Modeling of High-Frequency Electrical Conduction in Carbon Nanofibers, *IEEE Transactions on Electron Devices*, Vol. 56, No. 8, 2009, pp. 1557-1561.

[11] Liu, Y., Mandlis, A., Choy, M., Wang, C., and Segal, L., Remote Quantitative Temperature and Thickness Measurements of Plasma-Deposited Titanium Nitride Thin Coatings on Steel using a Laser Interferometric Thermoreflectance Optical Thermometer, *Review of Scientific Instruments*, Vol. 76, 2005, pp. 1-11.

[12] Duan, S., Wu, D.-Y., Xu, X., Luo, Y., Tian, Z.-Q., Structures of water molecules adsorbed on a gold electrode under negative potentials, *Journal of Physical Chemistry C*, Vol. 114, No. 9, 2010, pp. 4051-4056.

[13] Ju S.-P., A molecular dynamics simulation of the adsorption of water molecules surrounding an Au nanoparticle, *Journal of Chemical Physics*, Vol. 122, No. 9, 2005, pp. 94718-1-6.

[14] Lee, S., Staehle, R.W., Adsorption of water on gold, *Corrosion*, Vol. 52, No. 11, 1996, pp. 843-52.

[15] Wells, R.L., Fort, T., Jr., Adsorption of water on clean gold by measurement of work function changes, *Surface Science*, Vol. 32, No. 3, 1972., pp. 554-60.

[16] Beran, A., The Reflectance Behaviour of Gold at Temperatures up to 500 °C, *TMPM Tschermaks Mineralogische und Petrographische Mitteilungen*, Vol. 34, 1985 pp. 211-215.